Supporting Information

for

Multifunctional Nanoplatform Delivering Carbon Monoxide and Cysteine Protease Inhibitor to Mitochondria under NIR Light Enhanced Synergistic Anticancer Efficacy

Qi Tang,[a] Jing Liu,[a] Cheng-Bin Wang,[b] Lu An, [b] Hai-Lin Zhang,[a] Yi Wang,[a] Bing Ren,[a] Shi-Ping Yang,*[b] and Jin-Gang Liu*[a]

[a] Key Laboratory for Advanced Materials, School of Chemistry & Molecular Engineering, East China University of Science and Technology, Shanghai 200237, P. R. China, E-mail:
E-mail: liujingang@ecust.edu.cn

[b] Key Lab of Resource Chemistry of MOE & Shanghai Key Lab of Rare Earth Functional Materials, Shanghai Normal University, Shanghai 200234, P. R. China
E-mail: shipingy@shnu.edu.cn

Experimental section

Chemicals: All reagents used were purchased commercially and without further purification unless otherwise noted. tpy^{COOH} (2,2':6',2''-terpyridine-4'-carboxylic acid),[S1] {[(tpy^{COOH})Ru(pdo)(Cl)](PF_6)} (Ru-Cl),[S2] TPPPy·PF_6(4-(methylphosphonium)pyridine hexafluor-phosphate),[S3] cysteine proteases inhibitor (N-(benzyloxycarbonyl)-leucyl-glycine-nitrile),[S4] amine-modified N-GQDs (NH_2-N-GODs)[S5] and CO probe (FL-CO-1)[S6] were synthesized according to the literatures.

Characterization Techniques: All test instruments are referred to our previous report.[S2]

Synthesis of {[(tpy^{COOH})Ru(pdo)(inhibitor)](PF_6)$_2$} (Ru-inhibitor): [(tpy^{COOH})Ru(pdo)

(Cl)](PF$_6$) (769 mg, 1 mmol), AgBF$_4$ (390 mg, 2 mmol) and cysteine proteases inhibitor (606 mg, 2 mmol) were added into freshly distilled EtOH (60 mL). The resulting solution was wrapped by aluminum foil and refluxed for 6 h under N_2 atmosphere. After cooling to room temperature, filter off the solution to remove AgCl precipitates and the filtrate was dried with Na_2SO_4. Solvents were removed under reduced pressure, and the obtained residue was thoroughly washed with ethyl acetate (20 mL × 3), and the final orange-yellow product was dried at ambient temperature. Yield: 919.9 mg (88.7 %). **^{1}H NMR** (400 MHz, DMSO-*d*6): δ ppm 9.82 (d, J = 4.80 Hz, 1H), 9.30 (s, 2H), 9.06 (d, J = 7.76 Hz, 2H), 8.82 (d, J = 7.60 Hz, 1H), 8.61 (t, J = 5.04, 5.12 Hz, 1H), 8.34 (d, J = 7.64 Hz, 1H), 8.26 (t, J = 6.80, 6.76 Hz, 1H), 8.16 (t, J = 7.55, 7.81 Hz, 2H), 7.71(d, J = 6.24 Hz, 3H), 7.56 (d, J = 7.36 Hz, 3H), 7.35 (m, 5H), 5.03 (d, J = 8.46 Hz, 1H), 4.86 (d, J = 8.42 Hz, 1H), 4.20 (d, J = 4.72 Hz, 2H), 4.03 (q, J = 7.12 Hz, 1H), 1.50 (m, 1H), 1.31(m, 1H), 1.18 (t, J = 7.03, 7.06 Hz, 2H), 0.85 (d, J = 6.63 Hz, 3H), 0.79 (d, J = 6.52 Hz, 3H). **ESI-MS:** *m/z,* [M-H]$^+$: calculated 891.2, found 891.2.

Synthesis of {[(tpy^{COOH})Mn(CO)$_2$(Br)]} (tpy^{COOH}MnCO): tpy^{COOH} (110 mg, 0.4 mmol) and Mn(CO)$_5$Br (120 mg, 0.44 mmol) were added into CH_2Cl_2 (10 mL). The resulting mixture solution was wrapped by aluminum foil and stirred at room temperature under dark condition for 12 h. After that, the crude product was collected by centrifugation and washed with CH_2Cl_2 for three times to remove excess Mn(CO)$_5$Br. The final product tpy^{COOH}MnCO was dried at ambient temperature. Yield: 188.8 mg (95.3 %). **^{1}H NMR** (400 MHz, DMSO-*d*6): δ ppm 9.26 (d, J = 4.98 Hz, 1H), 8.96 (s, 1H), 8.91 (t, J = 8.28, 9.48 Hz, 1H), 8.82 (d, J = 4.12 Hz, 1H), 8.26 (t, J = 7.80, 7.41 Hz, 1H), 8.10 (s, 2H), 7.96 (t, J = 7.32, 7.36 Hz, 1H), 7.75 (t, J = 5.52, 5.96 Hz, 1H), 7.65 (t, J = 6.36, 6.44 Hz, 1H). **ESI-MS:** *m/z,* [M-2CO-Br+CH_3OH]$^+$: calculated 364.0, found 363.9.

Synthesis of {[(tpy^{COOH})Mn(CO)$_2$(TPPPy)](BF$_4$)} (TPPMnCO): tpy^{COOH}MnCO (234 mg, 0.5 mmol), TPPPy (221 mg, 0.5 mmol) and AgBF$_4$ (117 mg, 0.6 mmol) were added into 10 mL N, N-

dimethylformamide (DMF). The resulting mixture solution was wrapped by aluminum foil and stirred at 50 °C under dark condition for 6 h. After cooling to room temperature, the AgBr precipitates were removed by centrifugation, and excess H_2O was added to the supernatant to precipitate the final product, which was further washed with H_2O three times and dried at ambient temperature. Yield: 106.8 mg (25.8 %). **^{1}H NMR** (400 MHz, DMSO-*d*6): δ ppm 8.81 (d, J = 6.84 Hz, 1H), 8.65 (d, J = 7.20 Hz, 1H), 8.43 (s, 2H), 8.11 (t, J = 6.64, 6.82 Hz, 1H), 7.92 (t, J = 7.28, 6.97 Hz, 4H), 7.74 (m, 15H), 7.64 (t, J = 5.34, 5.76 Hz, 3H), 6.97 (s, 2H), 5.23 (d, J = 6.72 Hz, 2H). **ESI-MS:** *m/z,* [M-2CO-H]$^+$: calculated 685.2, found 685.2.

Synthesis of {Ru-inhibitor@TPPMnCO@N-GQDs}, Nanoplatform (1): [(tpy^{COOH})Ru(pdo)(inhibitor)]$(PF_6)_2$ (118 mg, 0.1 mmol) and [(tpy^{COOH})Mn(CO)$_2$(TPPPy)](BF_4) (166 mg, 0.2 mmol) were added to 20 mL of DMF, and activated with 1-ethyl-3-(3-dimethyl aminopropyl) carbodiimide (EDC)/N-hydroxysuccinimide (NHS), to which NH_2-N-GQDs aqueous solution (1.0 mg/mL, 20 mL) was added, and the solution was stirred at RT for 24 h in the dark. The solution was then dialyzed in a dialysis tube (1000 Da) for 48 h, and nanoplatform (**1**) was obtained by freeze-drying. **XPS**: Mn 2.24 wt.%; Ru 11.48 wt.%. **FT-IR** (KBr, cm^{-1}): 3417 (s), 3076 (w), 2938 (w), 2854 (w), 2027 (m), 1928 (m), 1646 (s), 1552 (s), 1468 (m), 1389 (s), 1260 (m), 1167 (w), 1122 (w), 1043 (w), 844 (s), 795 (w), 760 (m), 666 (w), 558 (m). **UV-vis DRS** (λ_{max}, nm): 220, 258, 276, 320, 507.

Detection of Extracellular and Intracellular CO Release: The method for detecting extracellular and intracellular CO release is similar to our previous report,[S2] with changing the stimulus from H_2O_2 to 808 nm laser.

Cell Culture, Cytotoxicity Assay and Mitochondial Co-Localization Experiment: The details of procedures were followed according to our previous report.[S2]

Detection of Mitochondrial Membrane Potential (MMP): After pre-incubated HeLa cells

with nanoplatform (**1**) or non-targeted Ru-inhibitor@MnCO@N-GQDs (100 μg/mL) for 4 h, the cells were washed twice with PBS buffer and then irradiated with an 808 nm NIR laser (1.5 W cm^{-2}) for 0 or 10 min and incubated for another 12 h. After that, the cells were incubated with 5, 5′, 6, 6′-tetrachloro-1, 1′, 3, 3′-tetraethyl-imidacarbocyanine iodide (JC-1, Beyotime, C2006) (12.5 μM) for 30 min. Cells were then washed three times with PBS buffer and finally imaged with serum-free medium. Pictures were recorded in the emission wavelength range of 500–550 nm (JC-1 monomer) and 560–650 nm (JC-1 aggregate), while excitation wavelengths were 488 nm and 525 nm, respectively. All parameters were kept constant in each sample.

Animal Model: The mice (BALB/c, female, five weeks old) were purchased from Shanghai JieSijie Laboratory Animal Co., Ltd. *All animal experiments were conducted in strict accordance with the protocal of the institutioanl Animal Protection and Animal Use Committee and approved by the Animal Ethics Committee of Shanghai Normal University.*

In Vivo Anticancer Experiments: The 4T1 cells were implanted in the right flank of mice by subcutaneous injection. Mice were randomly divided into five groups (n = 5) for in vivo anticancer studies when the average tumor volume was about 100 mm^3. The tumor-bearing mice were treated with (I) PBS as a control group, (II) Ru-inhibitor@N-GQDs + 808 nm laser, (III) Ru-Cl@TPPMnCO@N-GQDs + 808 nm laser, (IV) nanoplatform (**1**) without laser irradiation and (V) nanoplatform (**1**) + 808 nm laser (1.5 W/cm^2, 10 min) via intratumorally injected (40 mg/kg^{-1}). The mice in each group received only one treatment (single drug injection plus NIR light irradiation). The tumor size and mouse body weight were monitored every 2 days and the tumor volume was calculated by following the formula: $V = 0.5 \times L \times W^2$, where L and W represent the longest diameter and shortest diameter, respectively.[S7] After the treatment, the tumors in all mice were surgically removed and photographed. The tumors were then immersed in formalin for TUNEL, H&E and Ki-67 staining.

Statistical Analysis: All experimental data were performed at least three groups of independent tests, and the data were expressed as mean ± standard deviations (SD). Differences between groups were analyzed by one-step analysis of variance (ANOVA), $p < 0.05$ were considered to be statistically significant ($*p < 0.05$, $**p < 0.01$ and $***p < 0.005$).

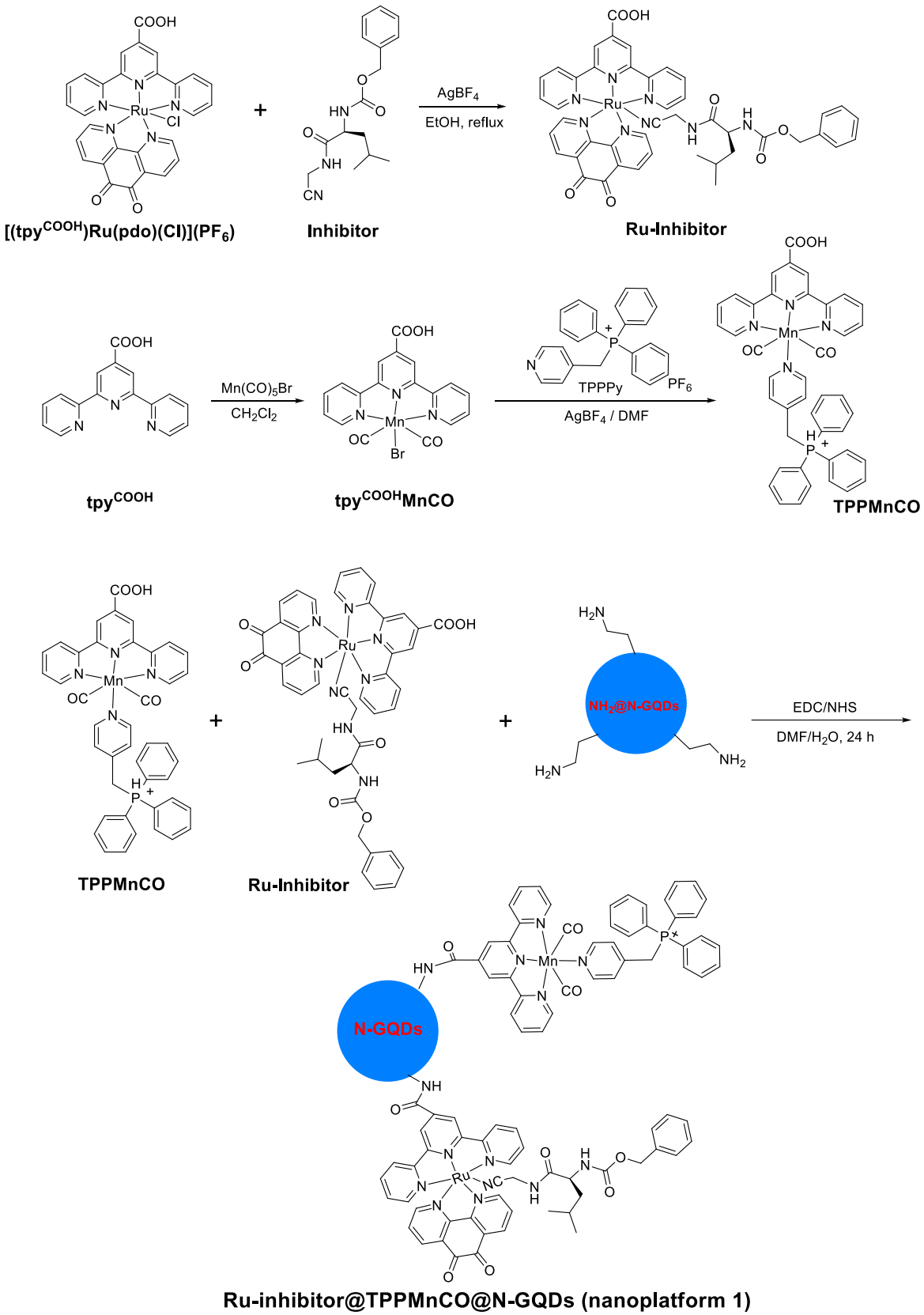

Scheme S1 Preparation procedure of nanoplatform (**1**).

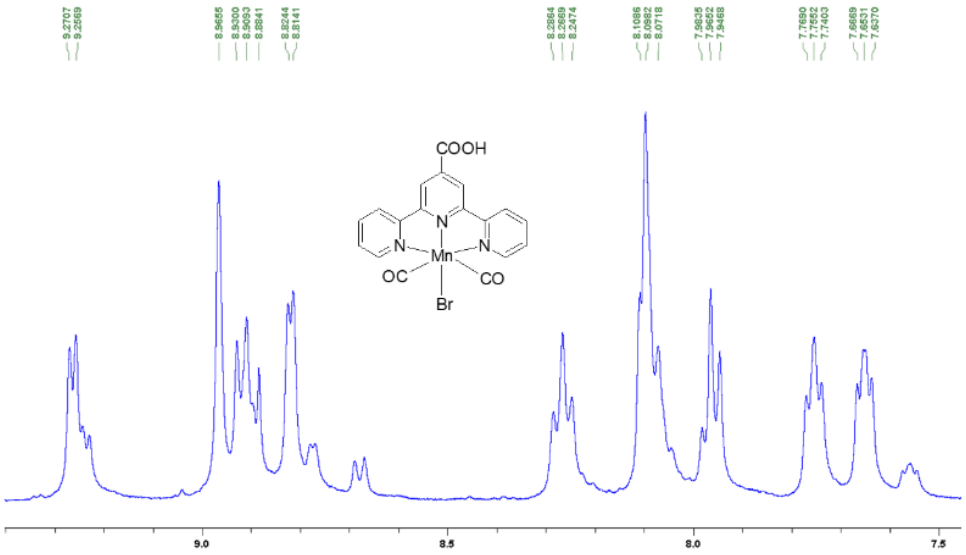

Fig. S1 ^{1}H NMR spectrum of [(tpy^{COOH})Mn(CO)$_2$(Br)] (tpy^{COOH}MnCO) in DMSO-*d*6.

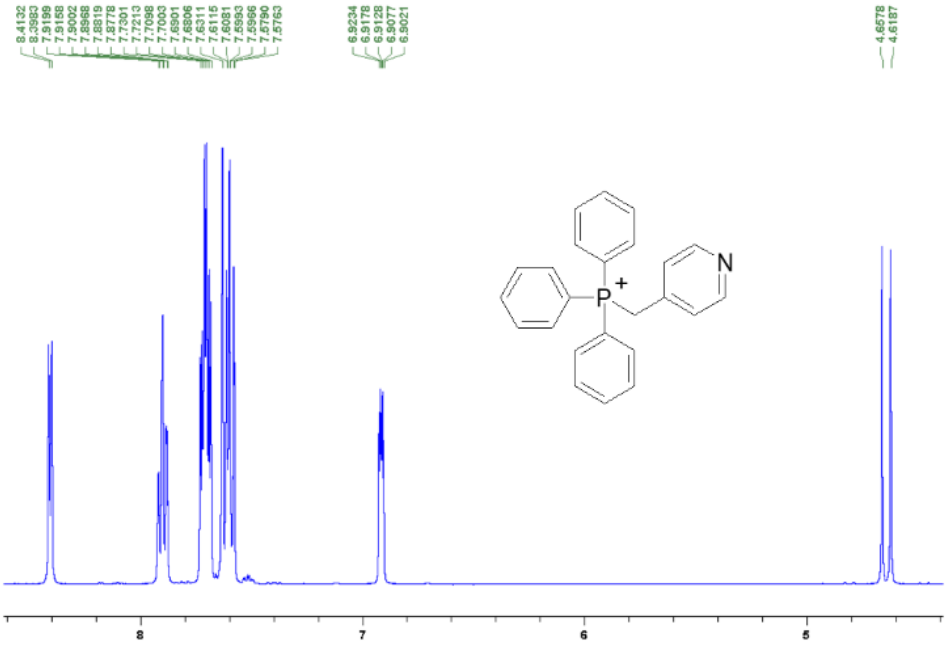

Fig. S2 ^{1}H NMR spectrum of TPPPy in CD_3CN-*d*3.

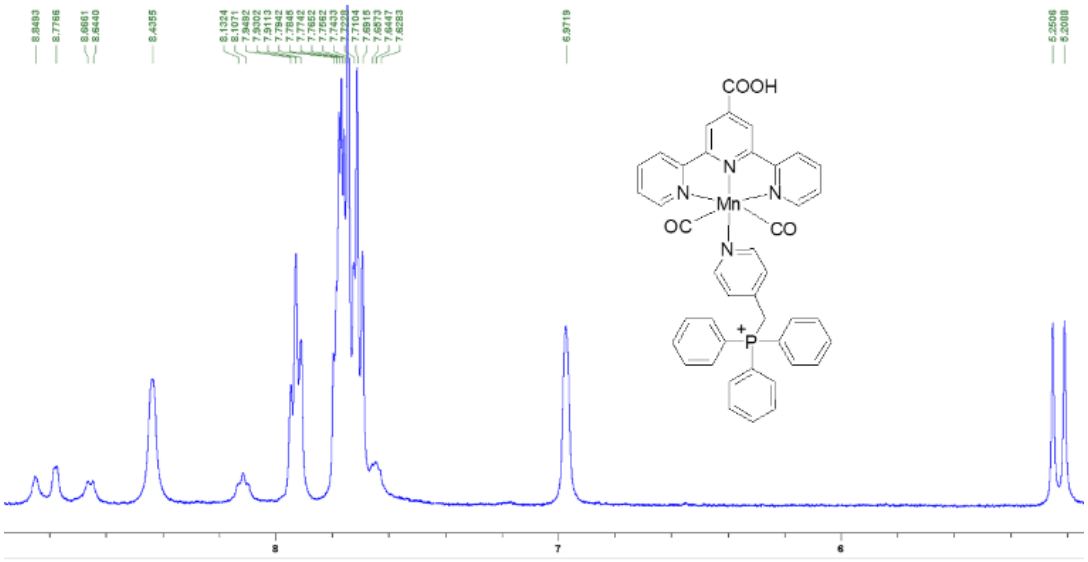

Fig. S3 ^{1}H NMR spectrum of [(tpy^{COOH})Mn(CO)$_2$(TPPPy)](TPPMnCO) in DMSO-*d*6.

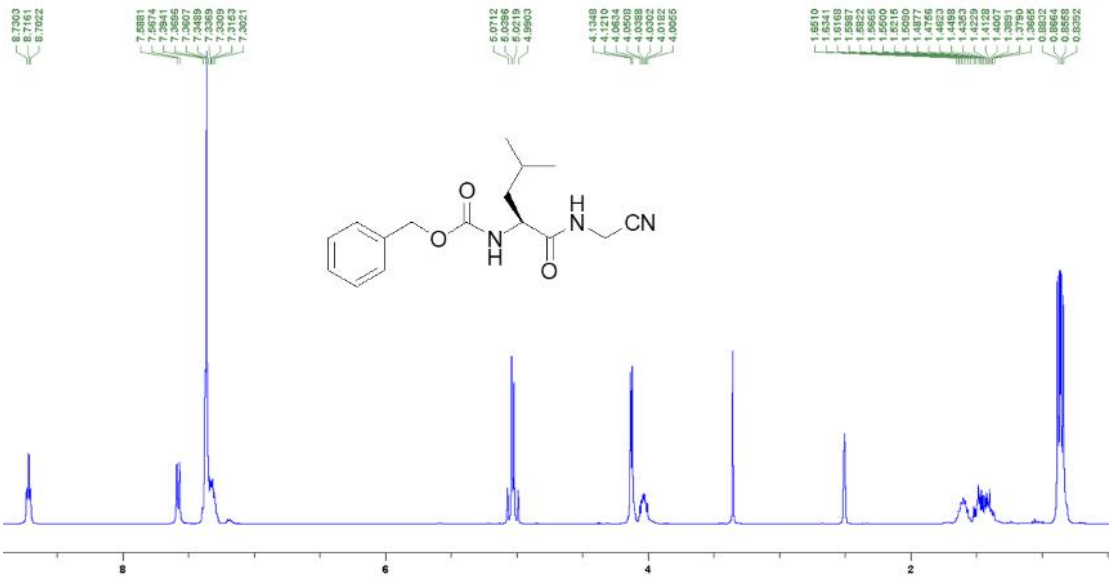

Fig. S4 ^{1}H NMR spectrum of cysteine protease inhibitor in DMSO-*d*6.

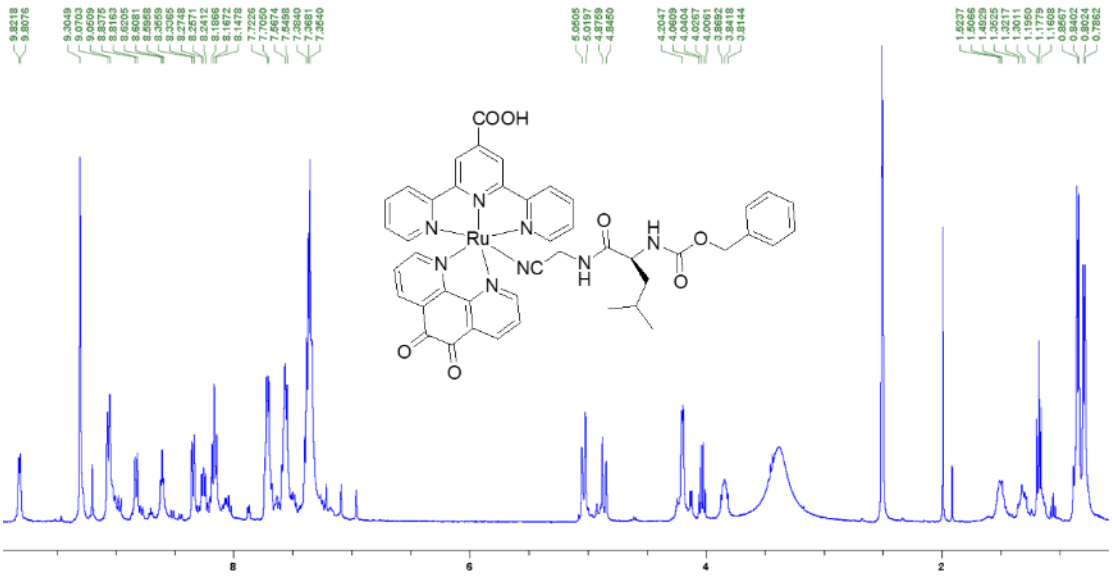

Fig. S5 ^{1}H NMR spectrum of {[(tpy^{COOH})Ru(pdo)(inhibitor)]} (Ru-inhibitor) in DMSO-*d*6.

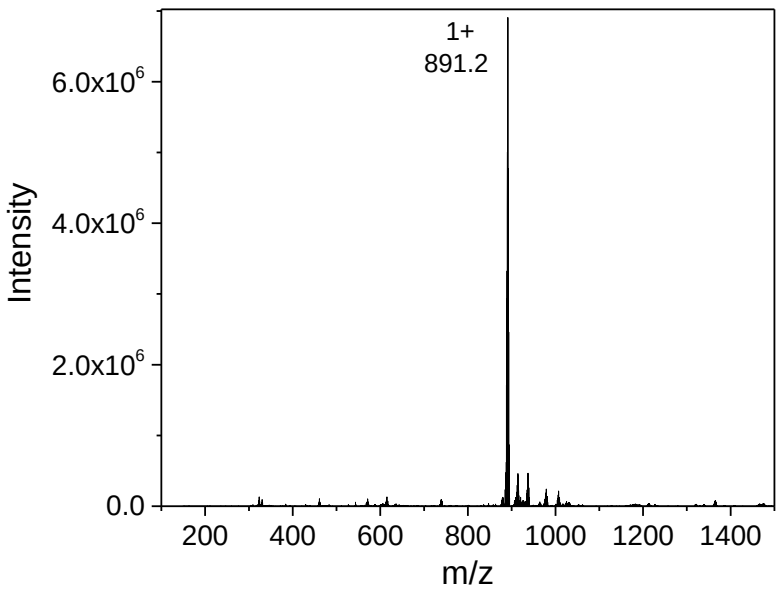

Fig. S6 ESI Mass spectrum of {[(tpy^{COOH})Ru(pdo)(inhibitor)]} (Ru-inhibitor).

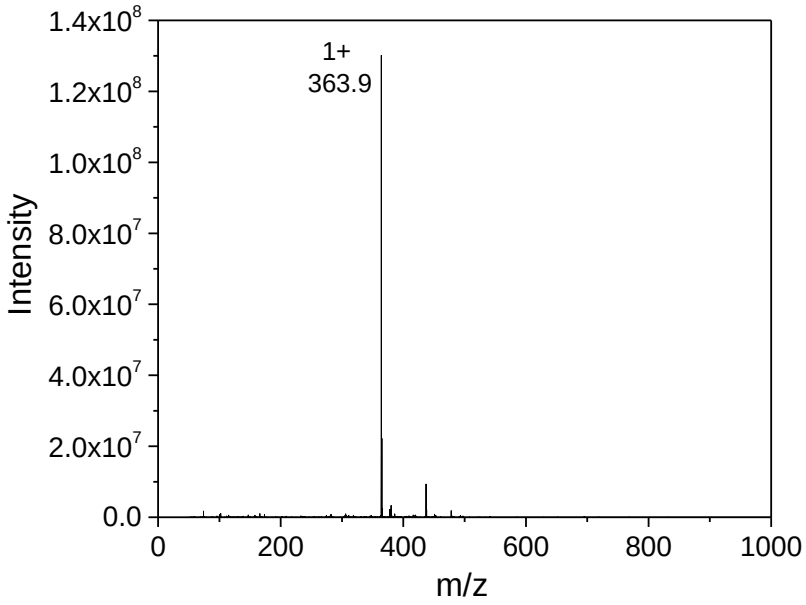

Fig. S7 ESI Mass spectrum of {[(tpy^{COOH})Mn(CO)$_2$(Br)]} (tpy^{COOH}MnCO).

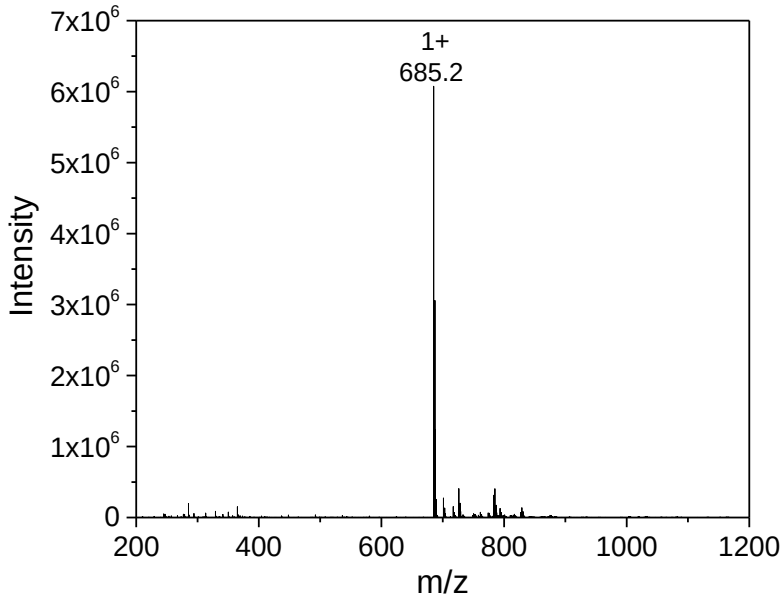

Fig. S8 ESI Mass spectrum of {[(tpy^{COOH})Mn(CO)$_2$(TPPPy)]}(TPPMnCO).

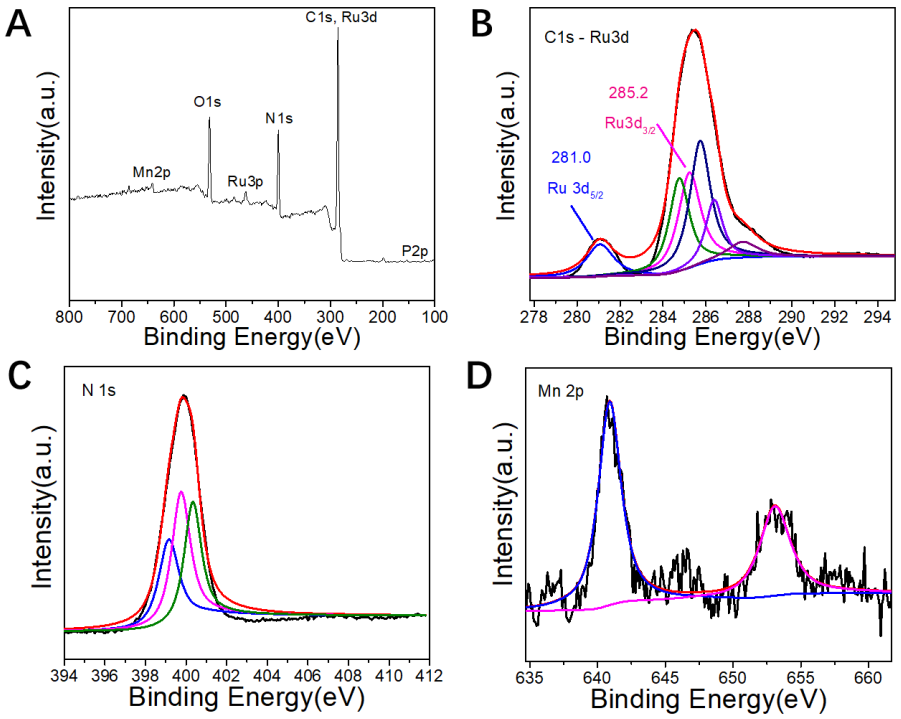

Fig. S9 XPS survey spectrum (A), High-resolution C 1s–Ru 3d (B), High-resolution N 1s (C) and High-resolution Mn 2p spectrum (D) of nanoplatform (**1**).

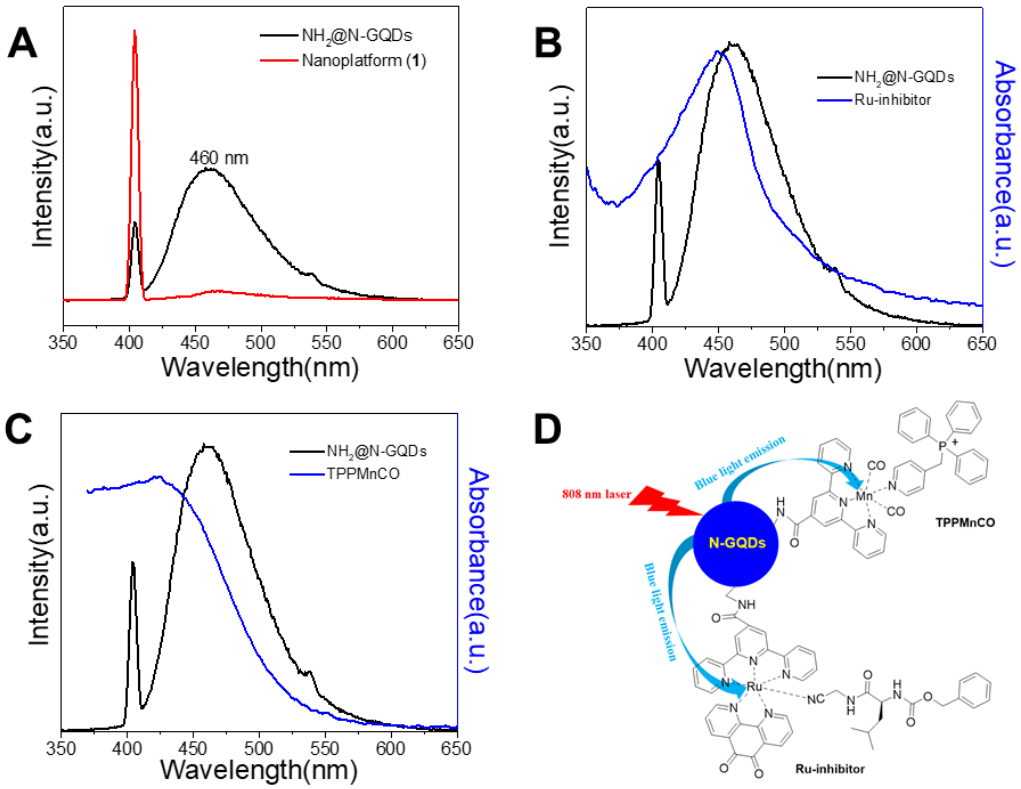

Fig. S10 (A)Up-conversion fluorescence spectrum of NH_2@N-GQDs (black line) and nanoplatform (**1**) (red line) (E_x = 808 nm). (B) Up-conversion fluorescence emission spectrum of NH_2@N-GQDs (black line) and UV-vis absorption spectrum of Ru-inhibitor. (C) Up-conversion fluorescence emission spectrum of NH_2@N-GQDs (black line) and UV-vis absorption spectrum of TPPMnCO. (D) Presumed mechanism of fluorescence resonance energy transfer (FRET) of nanoplatform (**1**).

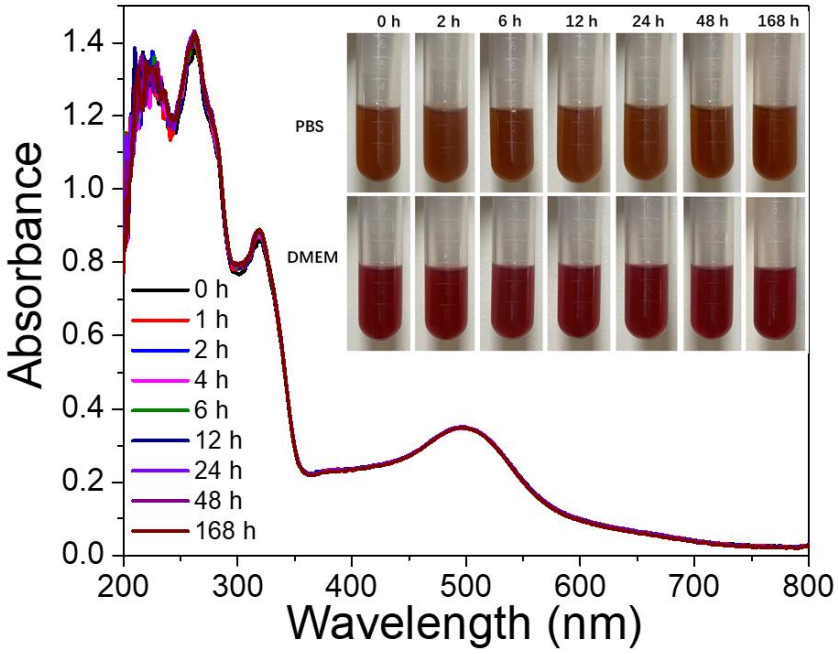

Fig. S11 The UV-vis spectrum of nanoplatform (**1**) under PBS buffer (pH=7.4) without 808 nm laser, with the inset showing its dispersion stability in PBS buffer and DMEM medium.

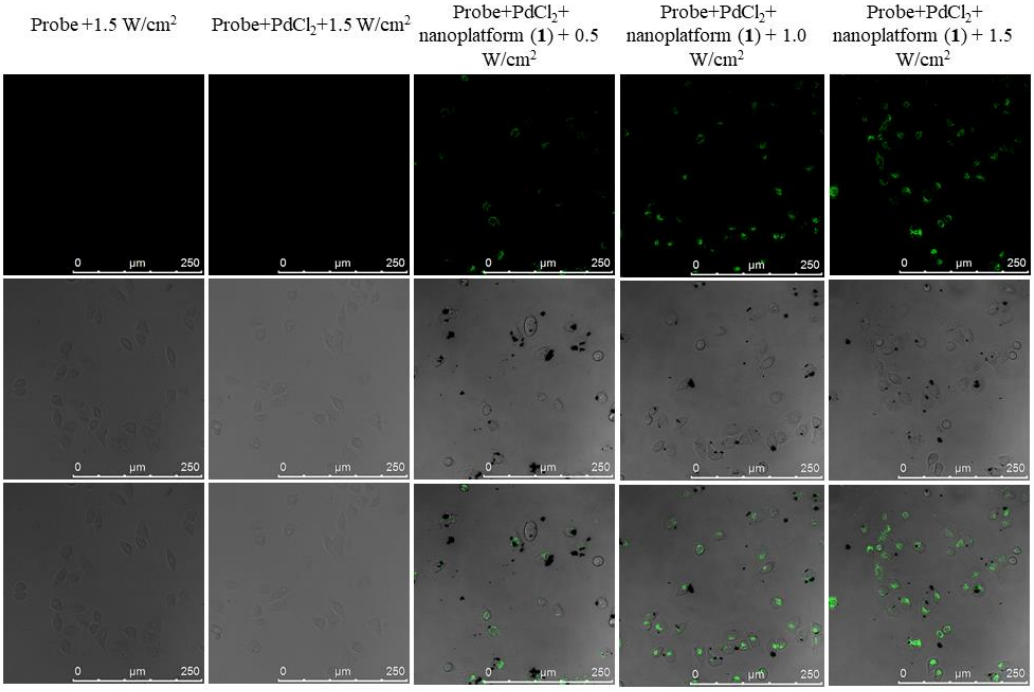

Fig. S12. Intracellular fluorescence image of CO by probe system (probe + $PdCl_2$, 5 μM each) upon 808 nm laser irradiation. Scale bar: 250 μm.

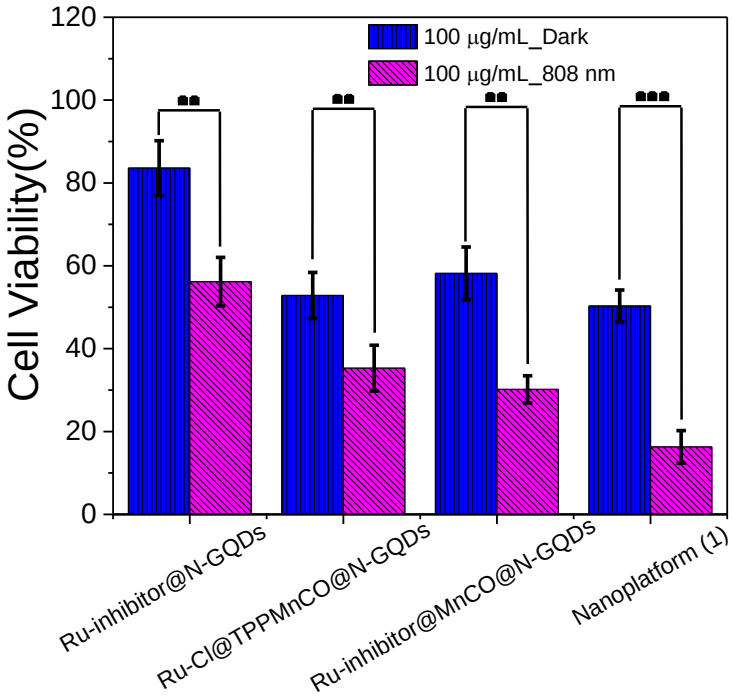

Fig. S13 Comparison of the lethality of 4T1 cells incubated with 100 μg/mL of Ru-inhibitor@N-GQDs, Ru-Cl@TPPMnCO@N-GQDs, Ru-inhibitor@MnCO@N-GQDs, or nanoplatform (**1**) in the presence or absence of 808 nm laser irradiation (1.5 W/cm^2, 10 min). (*$p < 0.05$, **$p < 0.01$, and ***$p < 0.005$).

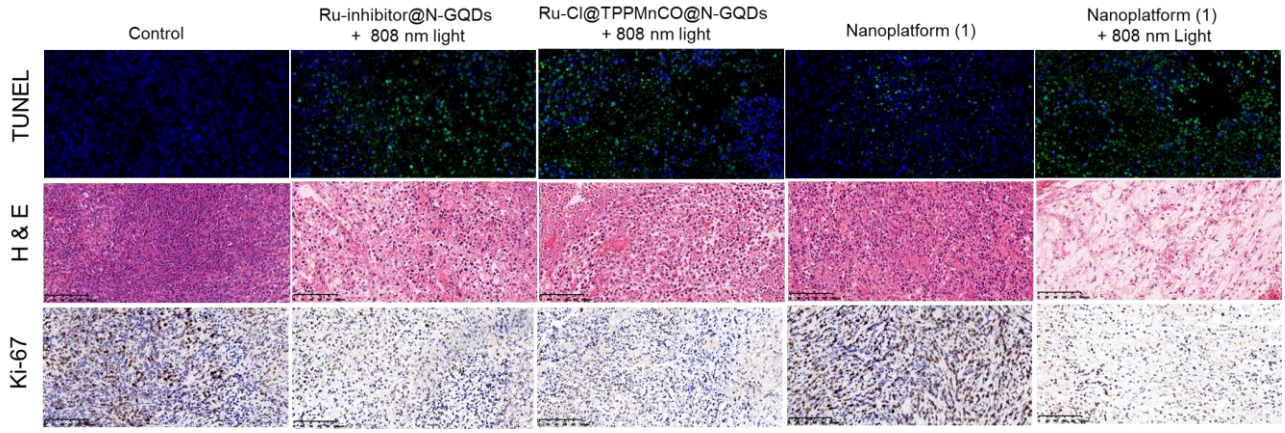

Fig. S14 TUNEL, H&E, and Ki-67 immunohistochemical staining of tumor tissue sections from each group.

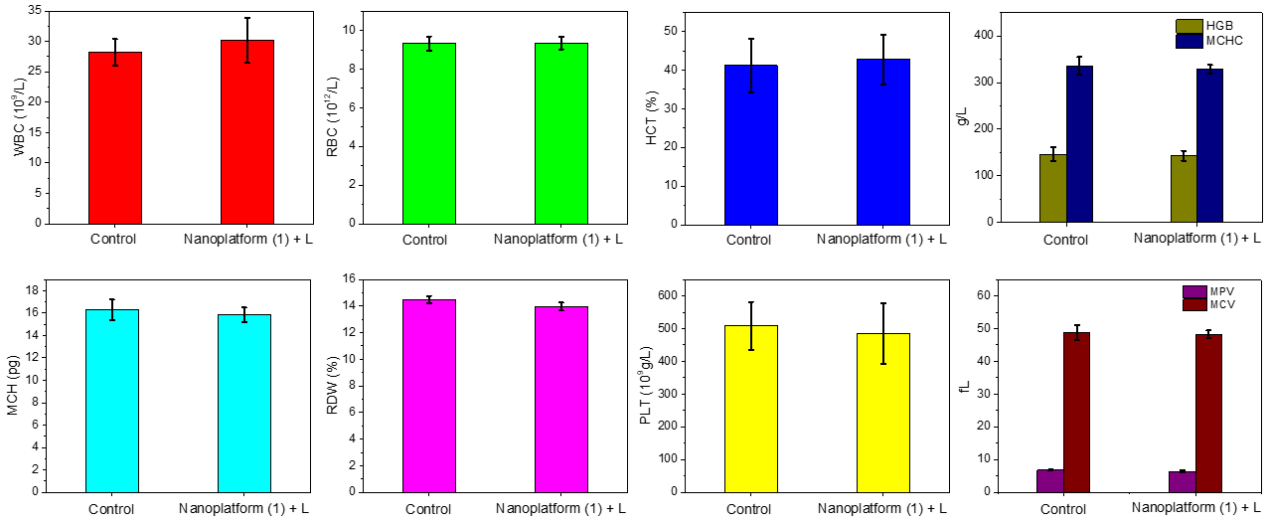

Fig. S15 The blood panel analysis test of mice after 14 days of treatment. (WBC=White Blood Cell; RBC=Red Blood Cell; HCT=Hematocrit; HGB=Hemoglobin; MCH=Mean Corpuscular Hemoglobin; MCHC=Mean Corpuscular Hemoglobin Concentration; RDW= Red Blood Cell Volume Distribution Width; PLT=Platelet; MPV=Mean Platelet Volume; MCV=Mean Corpuscular Volume)

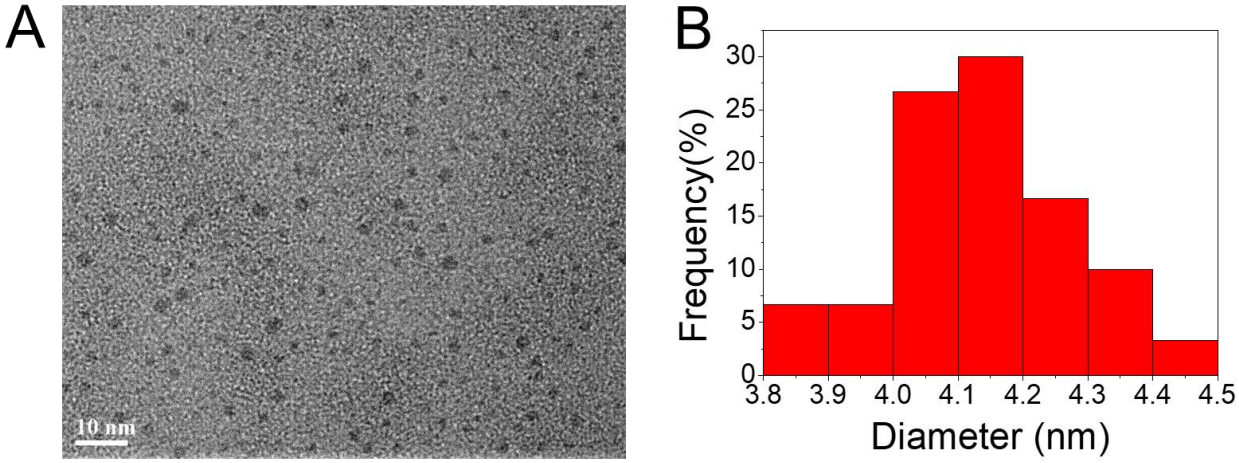

Fig. S16 (A) TEM image and (B) the size statistical distribution of nanoplatform (1).

Notes and references

S1 E. C. Constable, E. L. Dunphy, C. E. Housecroft, M. Neuburger, S. Schaffner, F. Schaper and S. R. Batten, *Dalton Trans.*, 2007, 4323-4332.

S2 Q. Tang, H.-L. Zhang, Y. Wang, J. Liu, S.-P. Yang and J.-G. Liu, *J. Mater. Chem. B*, 2021, **9**, 4241-4248.

S3 M. M. Burgoyne, T. M. MacDougall, Z. N. Haines, J. W. Conrad, L. A. Calhoun, A. Decken and C. A. Dyker, *Org. Biomol. Chem.*, 2019, **17**, 9726-9733.

S4 J. T. Palmer, C. Bryant, D.-X. Wang, D. E. Davis, E. L. Setti, R. M. Rydzewski, S. Venkatraman, Z.-Q. Tian, L. C. Burrill, R. V. Mendonca, E. Springman, J. McCarter, T. Chung, H. Cheung, J. W. Janc, M. McGrath, J. R. Somoza, P. Enriquez, Z. W. Yu, R. M. Strickley, L. Liu, M. C. Venuti, M. D. Percival, J.-P. Falgueyret, P. Prasit, R. Oballa, D. Riendeau, R. N. Young, G. Wesolowski, S. B. Rodan, C. Johnson, D. B. Kimmel and G. Rodan, *J. Med. Chem.*, 2005, **48**, 7520-7534.

S5 M. Guo, H.-J. Xiang, Y. Wang, Q.-L. Zhang, L. An, S.-P. Yang, Y. Ma, Y. Wang and J.-G. Liu, *Chem. Commun.*, 2017, **53**, 3253-3256.

S6 S. Feng, D. Liu, W. Feng and G. Feng, *Anal. Chem.*, 2017, **89**, 3754-3760.

S7 Y. Opoku-Damoah, R. Zhang, H. T. Ta and Z. P. Xu, *Biomater. Sci.*, 2021, **9**, 6086-6097.